

# A HIGH-RESOLUTION INTERFEROMETER FOR POLARIZATION MEASUREMENTS AT 9.4 Gc/s.

Takakiyo Kakinuma and Haruo Tanaka

Abstract :

A compound interferometer with 0.7 min. arc for polarization measurements at 9.4 Gc/s was completed at Toyokawa. It consists of the preexisting 16-element interferometer and a new 2-element interferometer, the total length being about 90 meters. A new type of phase switch using a ferrite switch and a turnstile junction is practically free from amplitude modulation. A completely linear phase shifter consisting of a single turnstile junction is used for phase adjustment. S/N ratios of various multiplying systems are discussed.

## 1. Introduction

The eclipse observation in 1958<sup>(1)</sup> showed that there are two small centers of polarization of different sense in a source of S component over a bipolar sunspot group and the degree of polarization decreases with decreasing frequency. In order to confirm these results, 16-element interferometer at 9.4 Gc/s was constructed two years ago.<sup>(2)</sup> It produces 2.2 min. arc beam and can measure the distributions of intensity and polarization of the radio emission on the solar disk. From continuous observations, it has been confirmed that there are two centers of polarization in a source near the central meridian, but the resolving power is not yet enough to resolve these two centers completely even near C. M.

The observation of the variation with the solar rotation of the sense and the degree of polarization of each center may be considered to be very important for finding the configuration of the magnetic field over the sunspot and searching the model of the source of S component. At 3.3 Gc/s, the phase-switched interferometer with 0.86 min. arc beam has been constructed to measure the polarization of S component at Stanford University<sup>(3)</sup> and at 2.8 Gc/s the compound interferometer with 0.5 min. arc beam is now being constructed at Ottawa, Canada.<sup>(4)</sup>

At Toyokawa, a compound interferometer at 9.4 Gc/s for the polarization measurements has been constructed. It consists of a 16-element interferometer and a 2-element interferometer and can measure the distributions over the solar disk of intensity and polarization of the slowly varying component simultaneously. 16-element interferometer can be electrically changed to the compound interferometer and the observations with both instruments are being carried out every day.

## 2. Antenna system

The principle of the compound interferometer was given by A. E. Covington and N. W. Broten.<sup>(5)(6)</sup> If the complex voltage pattern of two interferometers are  $S_1$  and  $S_2$  respectively, the power pattern of the compound interferometer is given by  $2 \operatorname{Re} (S_1 S_2^*)$ . Our interferometer consists of 16-element interferometer and 2-element interferometer, as shown in Fig. 1. The latter is placed to the west of the former on the same EW line.

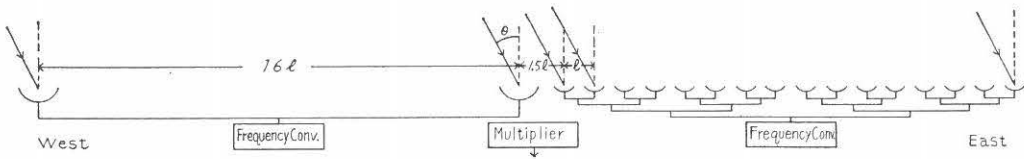
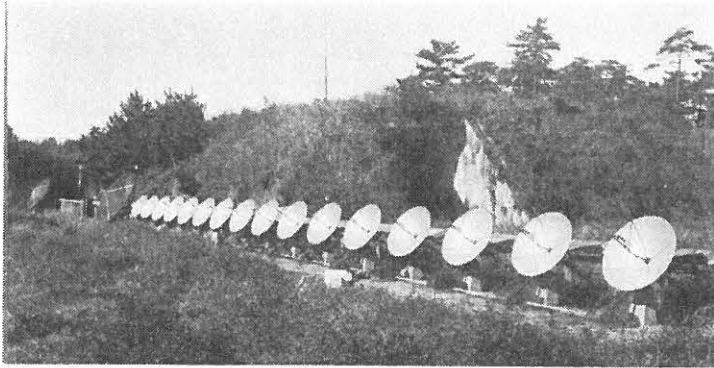


Fig. 1 (a). Formation of the compound interferometer

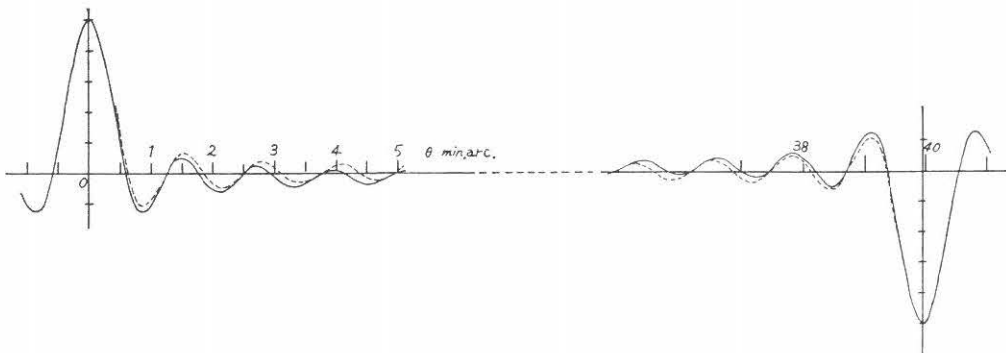


Fig. 1 (b). Normalized power pattern of the compound interferometer

Assuming that the spacing between two adjoining elements of the former is  $l$ , the spacing between two elements of the latter is  $16l$  and the spacing between the phase centers of two interferometers is  $17l$ . Instead of the last value,  $16l$  is preferable from the theoretical

point of view, but this is practically impossible to realize at the present wavelength. The power pattern is calculated as follows :

$$P(\theta, \phi) = 2(A(\theta, \phi) \sin 16x/4 \sin x) (\sqrt{2}B(\theta, \phi) \cos 16x) \cos 34x \\ = \sqrt{2}A(\theta, \phi) B(\theta, \phi) \sin 32x \cos 34x/4 \sin x$$

where  $A(\theta, \phi)$ : the voltage pattern of one element of 16-element interferometer

$B(\theta, \phi)$ : the voltage pattern of one element of 2-element interferometer

$l$  : spacing between two adjoining elements of 16-element interferometer  
2.74m

$\lambda$  : wavelength 3.18cm

$\theta$  : angle between the normal to EW line and the incoming ray

$x$  :  $\pi l \sin \theta / \lambda$ .

The normalized power pattern in  $\theta$  direction is shown in Fig. 1 (b). The half-power beamwidth is 0.7 min. arc. The dotted line is for the standard spacing between the phase centers of two interferometers, i. e. for  $16l$ . The effect of adding the length by  $l$  appears as a sinusoidal drift of the base line.

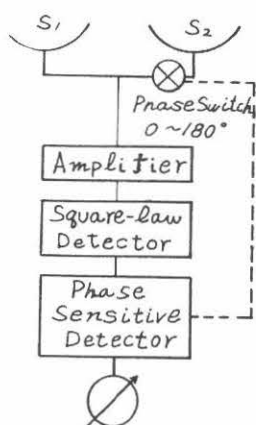


Fig. 2. Phase switching system

There are several methods for obtaining  $Re(S_1 S_2^*)$  from the outputs of two antennas,  $S_1$  and  $S_2$ .

At microwave frequencies around 3 Gc/s, a phase switch<sup>(7)</sup> or a rotary phase shifter<sup>(5)(6)</sup> is now being used in association with a square law detector and a phase sensitive detector, as shown in Fig. 2. One of the difficulties in this system seems to lie in obtaining a good phase switch. The problem of errors in the phase switching system was discussed in detail by G. Swarup.<sup>(7)</sup> If the phase switch produces an amplitude modulation,<sup>(7)(8)</sup> a spurious term which

The details of 16-element interferometer have been described by Tanaka.<sup>(2)</sup> Each element is a paraboloid antenna, 1.2m in diameter, with the feed for detecting circularly polarized components. The feed consists of  $H_{11}$  matched circular waveguide end and the ferrite switch with a quarter-wavelength plate. The outputs of 16 elements are combined in a conventional form with silver coated waveguide and magic tees. Each element of 2-element interferometer is a paraboloid antenna, 3m in diameter, with the same feed as the former and the outputs of the two antennas are combined in the same manner.

### 3. Multiplication system

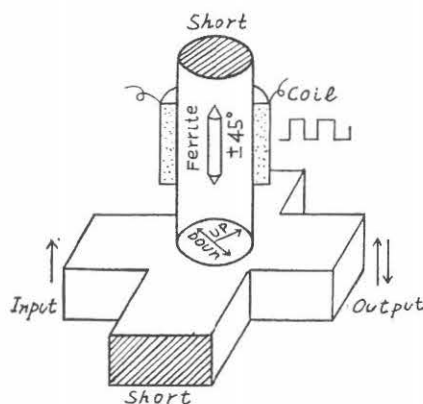


Fig. 3. Ferrite phase switch

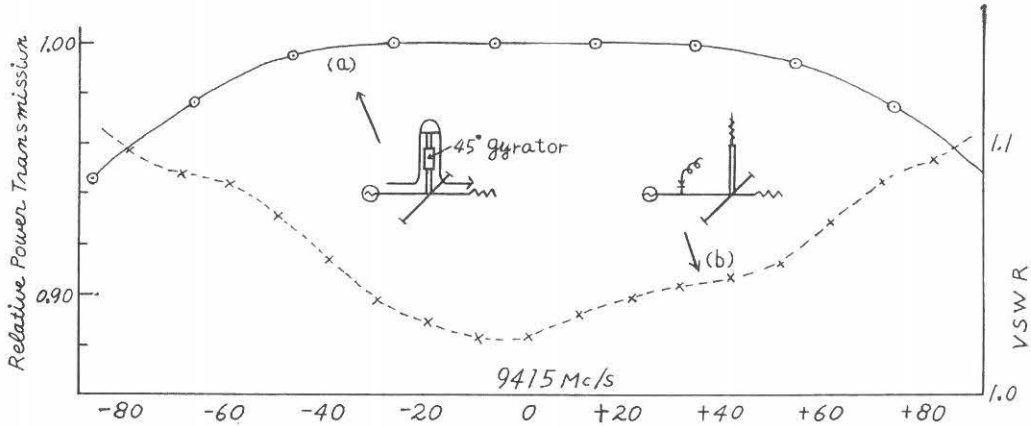


Fig. 4. Characteristics of ferrite phase switch. (a) Relative power transmission. (b) Matching characteristic of the junction showing a very small amount of the straight-going wave.

is proportional to the power response of one interferometer, i. e.  $S_2 S_2^*$  (in Fig. 2), will appear at the output of the phase sensitive detector. When the power response  $S_2 S_2^*$  is complex, it will be difficult to apply the correction to the record. For this reason, it is strongly desirable to make the amplitude modulation as small as possible for the polarization measurement where the signals are very weak.

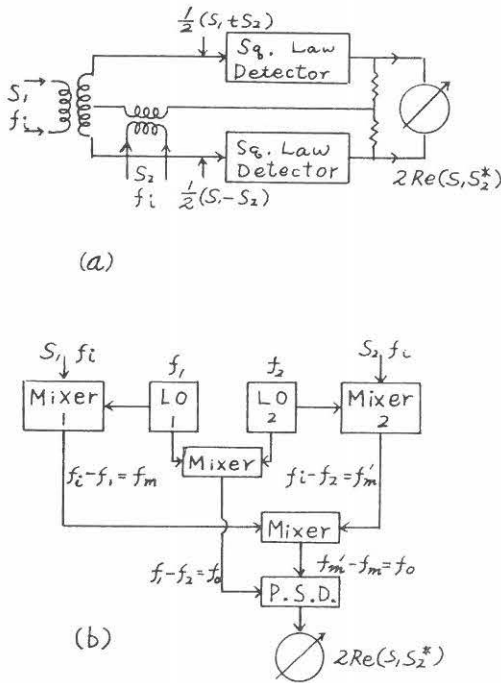


Fig. 5. Multipliers. (a) D. C. output multiplier. (b) A. C. output multiplier.

We have made a simple phase switch which seems to meet this requirement fairly well. As shown in Fig. 3, the phase switch consists of a turnstile junction and a  $\pm 45^\circ$  gyrator. Two rectangular arms of the turnstile junction are correctly short-circuited so as to produce linear polarization in the circular arm. The phase of the output wave reverses each time when the current of the field coil reverses. As the radio wave in each case goes through the same path, this phase switch produces little amplitude modulation at the center frequency. At the off-center frequency, a small fraction of the incoming wave will directly go to the output arm and this may produce an amplitude modulation. But as the turnstile junction has a very wide-band characteristics, we can neglect this effect for a frequency range of  $\pm 50$  Mc/s. The

characteristics of this phase switch are shown in Fig. 4.

In addition, the error in the rotation angle of the gyrator does not produce the phase error, though it increases the insertion loss. The equivalent waveguide length of the phase switch will vary with frequency. This variation produces the fixed phase error at the off-center frequency. But this variation is negligible for a frequency range of  $\pm 50$  Mc/s.

At lower frequencies, the above phase switching system and the electronic multiplying systems<sup>(9) (10) (12)</sup> as shown in Fig. 5(a) and (b) are used. In Fig. 5(a), D. C. output is proportional to  $\text{Re}(S_1 S_2^*)$ . The difficulty of this circuit will be to obtain two detectors of the same characteristics. If two detectors are unbalanced,  $S_1 S_1^*$  and  $S_2 S_2^*$  will appear at the output. On the other hand in Fig. 5(b), where  $S_2$  is converted to a frequency different from  $S_1$  and the component which has the difference frequency is picked up at the output of the mixer, these spurious terms do not appear on the record.

Now we have to compare S/N ratios of the above methods. The spectrum of the output of the square law detector or the mixer of the correlator has been calculated by Akabane.<sup>(12)</sup> In the two element interferometer,

$$S_2 = k S_1 (t + \tau_0), \quad \tau_0 = L \sin \theta / c$$

where  $L$  : distance between two antennas

$\theta$  : angle between the normal to EW line and the incoming ray

$c$  : light velocity

$k$  : constant, proportional to the ratio of antenna gain

and  $S_1$  and  $S_2$  are considered to be Gaussian noise.

The power spectrum of the output of the square law detector or the mixer in each case is as follows.

(1) D. C. output multiplier (Blum's multiplier)

$$\text{signal} : P_{S_1} P_{S_2} \rho^2(\tau_0) \cos^2 \varphi_0 \cdot 2\delta(f)$$

noise near D. C. ( $f \approx 0$ ,  $B - f \approx B$ ):

$$(P_{S_1} + P_{N_1})(P_{S_2} + P_{N_2})/B + (P_{S_1} P_{S_2} \sin 2\pi\tau_0 B / 2\pi\tau_0 B^2) \cos 2\varphi_0$$

where  $P_{S_1}$  and  $P_{S_2}$  : total power of  $S_1$  and  $S_2$  at the input of the multiplier, respectively

$P_{N_1}$  and  $P_{N_2}$  : total noise power of two receivers at the input of the multiplier, respectively

$B$  : bandwidth of the receivers

$\rho(\tau)$  : normalized correlation function  $\sin \pi B\tau / \pi B\tau$

$\varphi_0$  :  $2\pi L \sin \theta / \lambda$

$\lambda$  : wavelength of the solar radio emission.

(2) A. C. output multiplier (Fig. 5(b))

(a) when the mixer is of balanced type, as shown in Fig. 5(a),

$$\text{signal} : (P_{S_1} P_{S_2} \rho^2(\tau_0) / 2) \delta(f - f_0)$$

noise near  $f_0$  ( $B - f \approx B - f_0$ ):

$$(P_{S_1} + P_{N_1})(P_{S_2} + P_{N_2})(B - f_0) / B^2$$

(b) when the mixer consists of an adding circuit and a square law detector and  $f_0 \ll B$ ,

$$\text{signal} : 2P_{S_1} P_{S_2} \rho^2(\tau_0) \cdot \delta(f - f_0)$$

noise near  $f_0$ :

$$2(P_{S1} + P_{S2} + P_{N1} + P_{N2})^2 (B - f_0) / B^2 + P_{S1} P_{S2} 4 (B - f_0) \cos 2\pi f_0 \tau_0 / B^2$$

(c) if we use the same mixer as (b) and  $B \ll f_0 \ll f_m$  or  $f_m'$ ,

signal:  $2P_{S1} P_{S2} \rho^2(\tau_0) \cdot \delta(f - f_0)$

noise near  $f_0$ :

$$2(P_{S1} + P_{N1})(P_{S2} + P_{N2}) / B.$$

(3) Phase switching system

In this case, the signal voltage  $S$  at the input of the square law detector is  $(S_1 + AS_2) / \sqrt{2}$ , where  $A(t) = 1$  for  $t$  from 0 to  $T/2$ ,  $A(t) = -1$  for  $t$  from  $T/2$  to  $T$  and  $T$  is the period of the phase switch.

The spectrum of the output of the detector is calculated from the auto-correlation function of  $(S+N)^2$  and is as follows.

signal:  $(8P_{S1} P_{S2} \rho^2(\tau_0) \cos^2 \varphi_0 / \pi^2) \cdot \delta(f - f_0)$ ,  
 $T = 1 / f_0$

noise near  $f_0$  ( $f_0 \ll B$ ):

$$\begin{aligned} & (2P_N^2 + 2P_N P_{S1} + P_{S1}^2 / 2 + P_{S2}^2 / 2) (B - f_0) / B^2 \\ & + (8/\pi^2) (2P_N P_{S2} + P_{S1} P_{S2}) \{ (B - f_0) / B^2 \\ & + (B - 3f_0) / 9B^2 + \dots \} + (8/\pi^2) P_{S1} P_{S2} \cos 2\varphi_0 \\ & \{ \{ \sin 2\pi\tau_0 B + \sin 2\pi\tau_0 (B - 2f_0) \} / 4\pi\tau_0 B^2 \\ & + \{ \sin 2\pi\tau_0 (B - 2f_0) + \sin 2\pi\tau_0 (B - 4f_0) \} \\ & / 9 \cdot 4\pi\tau_0 B^2 + \dots \} + P_{S1} P_{S2} (B - f_0) \cos 2\pi\tau_0 f_0 / B^2. \end{aligned}$$

In the systems (2) and (3), we have to calculate the spectrum near D. C. of the output of the phase sensitive detector. In our interferometer, the noise figure of the receiver is  $\sim 10$  and the equivalent antenna temperature of the signal is estimated

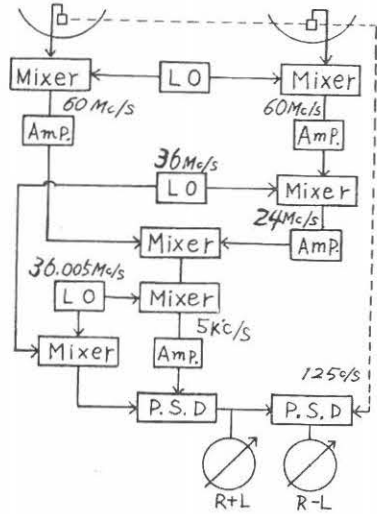


Fig. 6. Block diagram of multiplier for experiment

to be  $2 \sim 300^\circ K$ . So we can assume  $P_N \gg P_S$  and will be able to neglect the terms including  $P_S$  in the above noise spectrum, compared with the term  $P_N^2$ . If we neglect these terms and so neglect the cross-correlation between signal and noise\*, the spectrum of the output

\* This consideration will be unnecessary for the intensity measurement, but as the polarization signal is the difference between two intensity signals, we can not neglect these terms when  $P_S \geq P_N$ .

For example, the power spectrum of the output of the phase sensitive detector in the system (2, a) is calculated as follows.

signal:  $\frac{1}{\pi^2} P_{S1} P_{S2} \rho^2(\tau_0) \cos^2 \varphi_0$

noise near D. C.:  $\frac{(2B - 2f_0 - f)}{\pi^2 B^2} (P_{S1} + P_{N1}) \times$

$(P_{S2} + P_{N2}) + \frac{1}{\pi^2} P_{S1} P_{S2} \frac{\sin \{2\pi (B - f) \tau_0\}}{2\pi B^2 \tau_0} \cos 2\varphi_0$

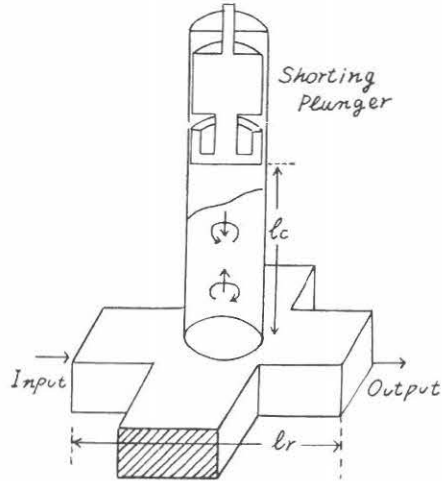


Fig. 7. Turnstile phase shifter

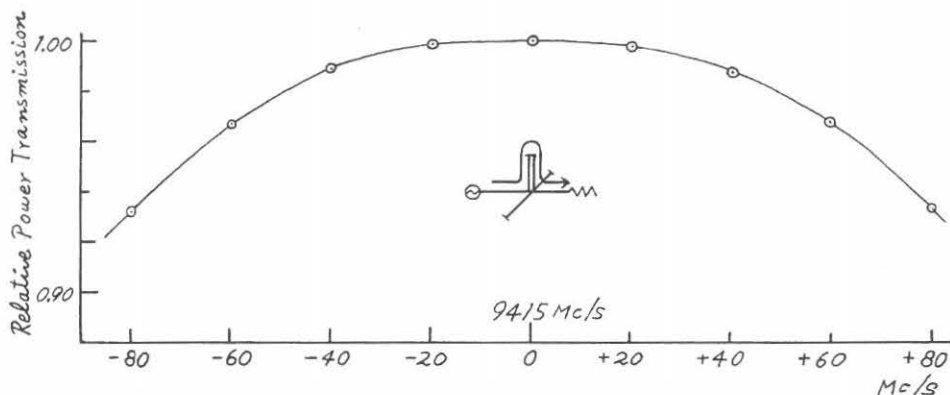


Fig. 8. Frequency characteristic of the turnstile phase shifter

of the phase sensitive detector for the half-wave rectification is calculated as follows.

Signal (D. C.):  $(A^2/\pi^2) 2\delta(f)$

Noise near D. C.:

$$2P_{N'}/\pi^2b$$

where  $A$  : amplitude of  $f_0$  component

$P_{N'}$  : total noise power at the input

$b$  : bandwidth of the selective amplifier

S/N ratio :  $A^2 b/2 P_{N'} \cdot W$

$W$  : bandwidth of the low pass filter.

Accordingly we obtain the following conclusion:

$$(S/N)_{(1)} = (S/N)_{(2,c)} > (S/N)_{(2a)} > (S/N)_{(3)} > (S/N)_{(2b)}$$

The system (2, c) has the best (S/N) ratio, as well as the system (1). In addition, the system (2, c) has the merit of producing no spurious terms on the record. But we need two separate i-f amplifiers and we should adjust these amplifiers of different center frequency to have the same bandshape and bandwidth.

When we choose the system (3), we also need two i-f amplifiers, because the transmission loss of the waveguide is large at 9.4 Gc/s and so we have to convert both signals to i-f frequency. But these amplifiers have the same center frequency and are easy to adjust. And as we can use the ferrite phase switch in one of the transmission lines of the local oscillator power, there is no transmission loss due to the phase switch. Furthermore, the errors in the phase of the phase sensitive detector do not produce the asymmetrical beam.<sup>(7)</sup> Therefore, although the S/N ratio is worse than the system (2, c), there seem fewer troubles in the phase switching system.

After these discussions, we have decided to test both systems. The block diagram of the system (2, c) is shown in Fig. 6.

#### 4. Phase adjustment

The phase of the 2 element interferometer is not easy to adjust. First, the electrical

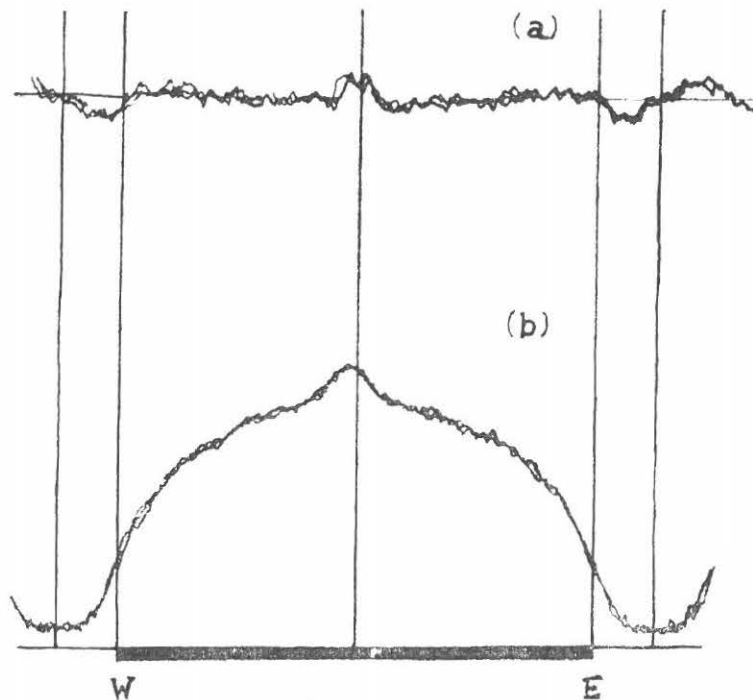


Fig. 9. Three superposed scan curves on Jan. 16, 1962, obtained with  
 (a) the compound interferometer  
 (b) 16-element interferometer.

length from the feeds of the 3-meter dishes to the output were balanced step by step by the short-circuit method. Then final adjustment was made by observing the drift curve.

A phase shifter using turnstile junction<sup>(3)</sup> is very convenient for this purpose. Fig. 7 is the sketch of the phase shifter, where the input wave enters the circular waveguide in right-hand sense, which is reflected in left-hand sense and thus goes through the output arm. According to our experiment, the equivalent waveguide length of this phase shifter is approximately  $l_r + 2(\lambda_r/\lambda_c)l_c$ , where  $\lambda_r$  and  $\lambda_c$  are wavelengths in rectangular and circular waveguides respectively. This means that the change of electrical length by a frequency change is completely balanced by a rectangular waveguide of equivalent waveguide length within a frequency range of more than  $\pm 40$  Mc/s. Linearity is perfect and the insertion loss is less than 1% within a frequency range of  $\pm 37$  Mc/s. The results of our experiments are shown in Fig. 8.

An example of the scan curves obtained with the system (3) is shown in Fig. 9. As the sun is very quiet now, we can not yet confirm the sharpness of the beam, but the observed scan curve for the quiet sun is nearly consistent with the calculated one, based on the scan curve of 16-element interferometer. The system (2, c) has not yet completed.

As seen in Fig. 9, the compound interferometer has less sensitivity for the quiet sun component at this frequency. This will be convenient for the study of the localized



radio active regions.

## 5, Acknowledgement

The authors wish to express their thanks to Messrs. T. Torii, Y. Tsukiji and to all the staff of the Radio Astronomy Section here for their cooperation in constructing the interferometer. Finally, the authors wish to express their sincere thanks to Director, Professor A. Kimpara for his unceasing encouragement.

## References

- (1) H. Tanaka and T. Kakinuma: Rep. Ionosph. Res. Japan, 12, 3 (1958).
- (2) H. Tanaka: Proc. Res. Inst. Atmosph. Nagoya Univ. 8 (1961).
- (3) G. Swarup: private communication.
- (4) A. E. Covington: Bull. Radio Elec. Eng. Div. N. R. C. Canada, 11, 1 (1961).
- (5) A. E. Covington and N. W. Broten: I. R. E. Trans. AP-5, 3 (1957).
- (6) A. E. Covington: Jour. R. A. S. C., 54, 1 (1960).
- (7) G. Swarup: Sci. Rep. 13, Stanford Elec. Lab., Stanford Univ. (1962).
- (8) A. E. Covington, G. A. Harvey and H. W. Dodson: Ap. J., 135, 2 (1962).
- (9) R. Hanbury Brown, H. P. Palmar and A. R. Thomson: Phil. Mag. 46, (1955).
- (10) E. J. Blum: Ann. d'Astrophys., 22, 2 (1959).
- (11) S. Suzuki: Pub. Astr. Soc. Japan, 4, 11, 195 (1959).
- (12) K. Akabane: Res. Rep. EE 461, Elec. Eng. Cornell Univ. (1960).
- (13) S. Yoshida: Jour. Inst. Elec. Com. Eng. Japan, 35, 10 (1952).

